

Supplementary Materials for

Sea ice variability in the southern Norwegian Sea during glacial Dansgaard-Oeschger climate cycles

Henrik Sadatzki*, Trond M. Dokken, Sarah M. P. Berben, Francesco Muschitiello, Ruediger Stein, Kirsten Fahl, Laurie Menviel, Axel Timmermann, Eystein Jansen

*Corresponding author. Email: henrik.sadatzki@uib.no

Published 6 March 2019, *Sci. Adv.* **5**, eaau6174 (2019)
DOI: 10.1126/sciadv.aau6174

This PDF file includes:

Table S1. Tie points for the age model of core MD99-2284.

Fig. S1. Age model of core MD99-2284 32 to 40 ka ago.

Fig. S2. Tephra data supporting the age model of core MD99-2284.

Fig. S3. Supplementary biomarker proxy records from core MD99-2284.

Fig. S4. Proxy-model data comparison.

Table S1. Tie points for the age model of core MD99-2284.

MD99-2284 core depth cm	NGRIP age _{GICC05} ka b2k	Stratigraphy	Sedimentation rate cm/ka
1595.00	28.89	Onset of GI4	
2070.50	32.04	Termination of GI5	151.0
2120.50	32.51	Onset of GI5	106.4
2220.00	33.36	Termination of GI6	117.1
2340.50	33.73	Onset of GI6	325.7
2498.50	34.74	Termination of GI7	156.4
2684.50	35.49	Onset of GI7	248.0
2805.50	36.59	Termination of GI8	110.0
3041.00	38.081 ^a	Tephra (FMAZ III)	
3084.50	38.21	Onset of GI8	172.2
3185.50	39.93	Termination of GI9	58.7
3286.50	40.16	Onset of GI9	439.1 (213.2) ^b

^a Age is derived from the NGRIP ice core (43), but was not used for the age model.

^b Note that 213.2 cm/ka is the average sedimentation rate for GI5, 6, 7, and 8 and was used for flux calculations (fig. S1).

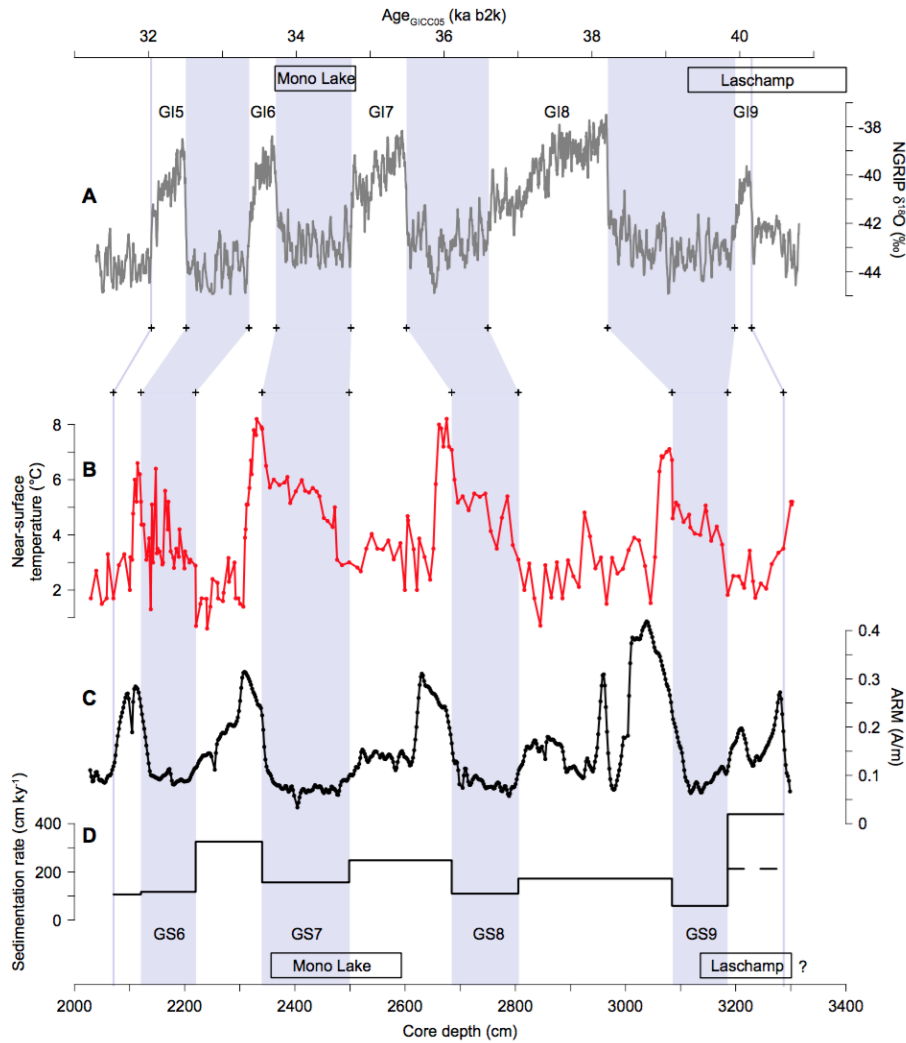


Fig. S1. Age model of core MD99-2284 32 to 40 ka ago. (A) NGRIP ice core $\delta^{18}\text{O}$ plotted as 11-point running average on the GICC05 b2k timescale (2, 4). (B) Near-surface temperature based on transfer function estimates using planktic foraminifera census counts (14). (C) Anhysteretic remanent magnetization (ARM) (14). (D) Sedimentation rate. (B)–(D) are plotted on the MD99-2284 core depth scale. Crosses mark tie points used for the age model. Boxes at top and bottom indicate positions of the Mono Lake and Laschamp events. GI, Greenland interstadials numbered at top. GS, Greenland stadials numbered at bottom (shaded bars). Note that the sedimentation rate for GI9 is probably biased by artificial stretching at the core bottom; therefore, the average interstadial sedimentation rate (averaging that of GI5, 6, 7, and 8; dashed line) was used to calculate biomarker fluxes (table S1).

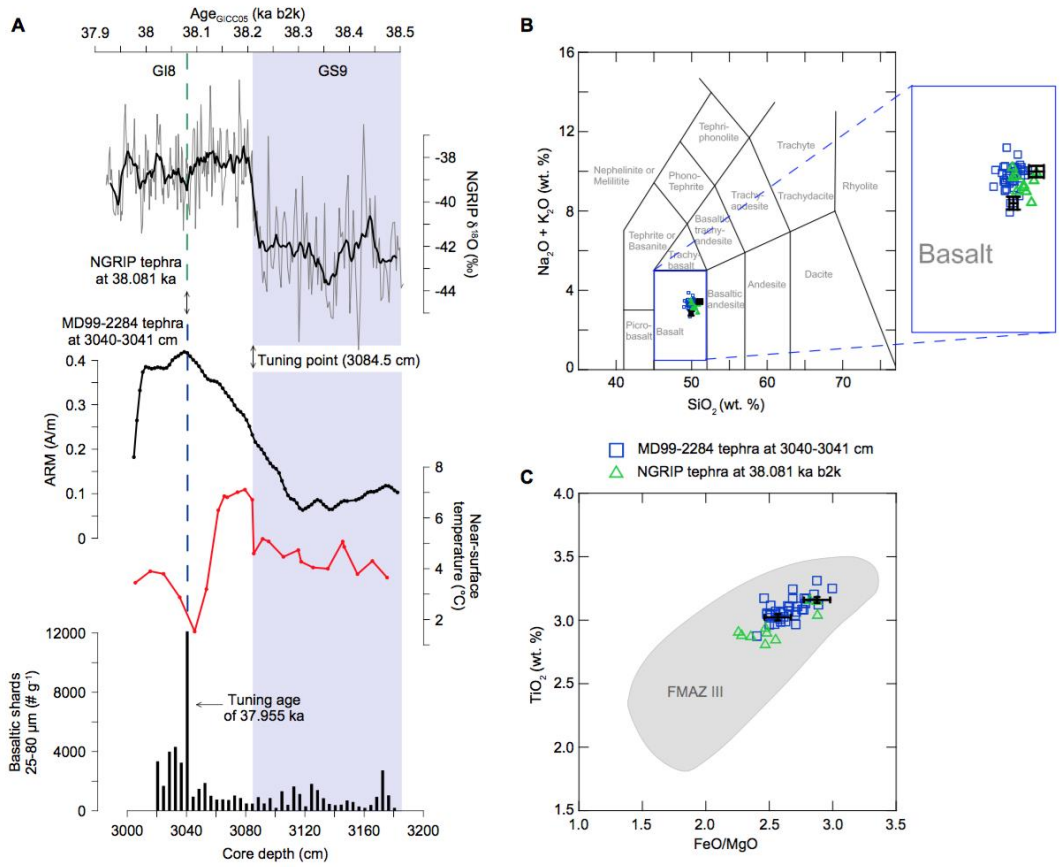


Fig. S2. Tephra data supporting the age model of core MD99-2284. (A) Top to bottom: NGRIP ice core $\delta^{18}\text{O}$ plotted on the GICC05 b2k timescale (black line is the 11-point running average) (2, 4), anhysteretic remanent magnetization (ARM) (14), near-surface temperature based on transfer function estimates using planktic foraminifera census counts (14), basaltic cryptotephra shard counts. ARM, near-surface temperature and cryptotephra shard counts are plotted on the MD99-2284 core depth scale that is aligned to the GICC05 timescale using the GS9–GI8 tuning point and is floating in deeper and shallower parts. Dashed green line, tephra layer identified in the NGRIP ice core at 2065.65 m (38.081 ka b2k) (42, 43). Dashed blue line, tephra layer identified in MD99-2284 at 3040–3041 cm. Greenland interstadial (GI) 8 and Greenland stadial (GS) 9 (shaded bar) indicated at top. (B) Total alkali versus silica diagram for the tephra layer at 3040–3041 cm (25–80 μm) in MD99-2284 (blue squares) and that at 2065.65 m in the NGRIP ice core (green triangles) (42). (C) FeO/MgO vs. TiO₂ biplot for the tephra layer at 3040–3041 cm (25–80 μm) in MD99-2284 (blue squares) and that at 2065.65 m in the NGRIP ice core (green triangles) (42). Shaded area indicates the compositional range of the Faroe

Marine Ash Zone III (FMAZ III) (58). Geochemical data were plotted on a normalized anhydrous basis. Black data points and uncertainty intervals in (B) and (C) are based on replicate analyses of the BCR2g reference glass.

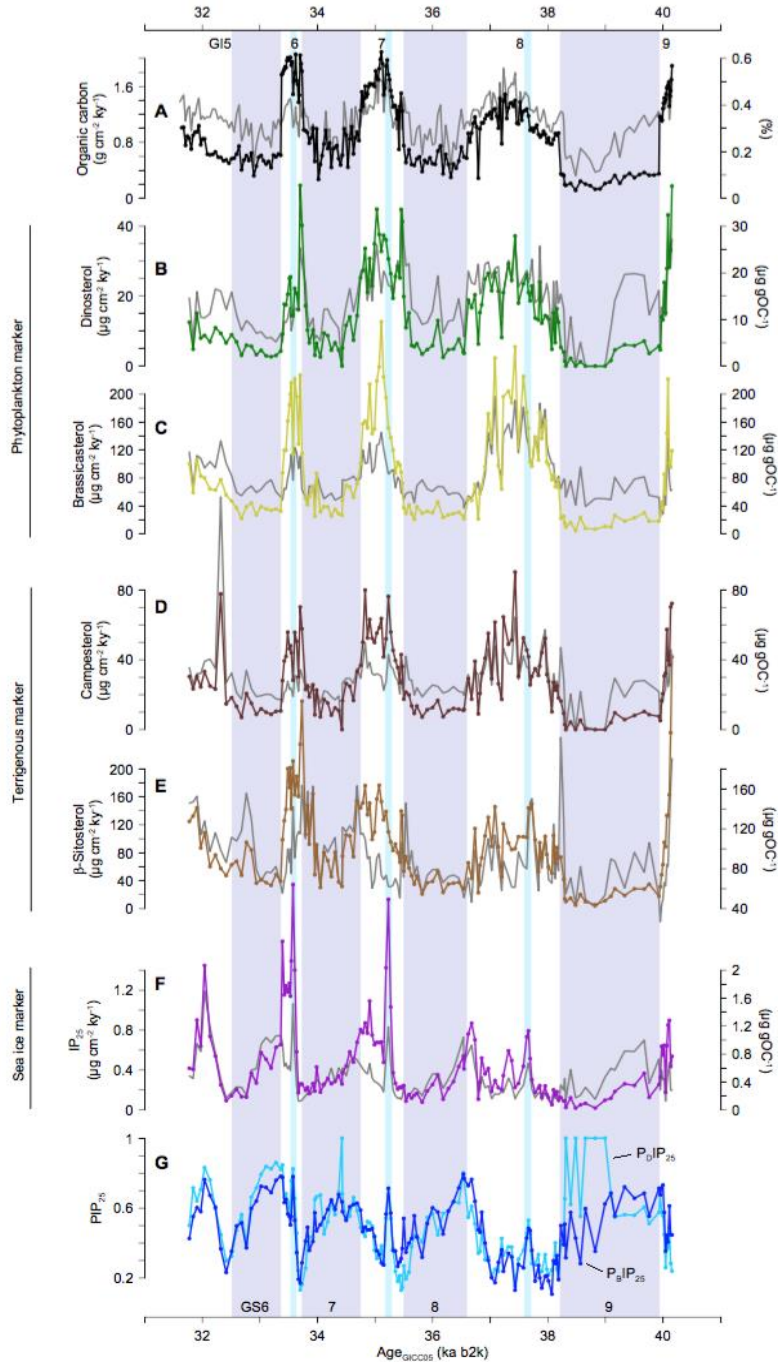


Fig. S3. Supplementary biomarker proxy records from core MD99-2284. (A) Organic carbon. (B) Dinosterol. (C) Brassicasterol. (D) Campesterol. (E) β-sitosterol. (F) IP₂₅. (G) P_DIP₂₅ and P_BIP₂₅. (A)–(F) shown as fluxes (colored) and concentrations (gray). All records are plotted on the GICC05 b2k timescale. GI, Greenland interstadials numbered at top. GS, Greenland stadials numbered at bottom (shaded bars). Light blue bars, intra-interstadial sea ice expansion events.

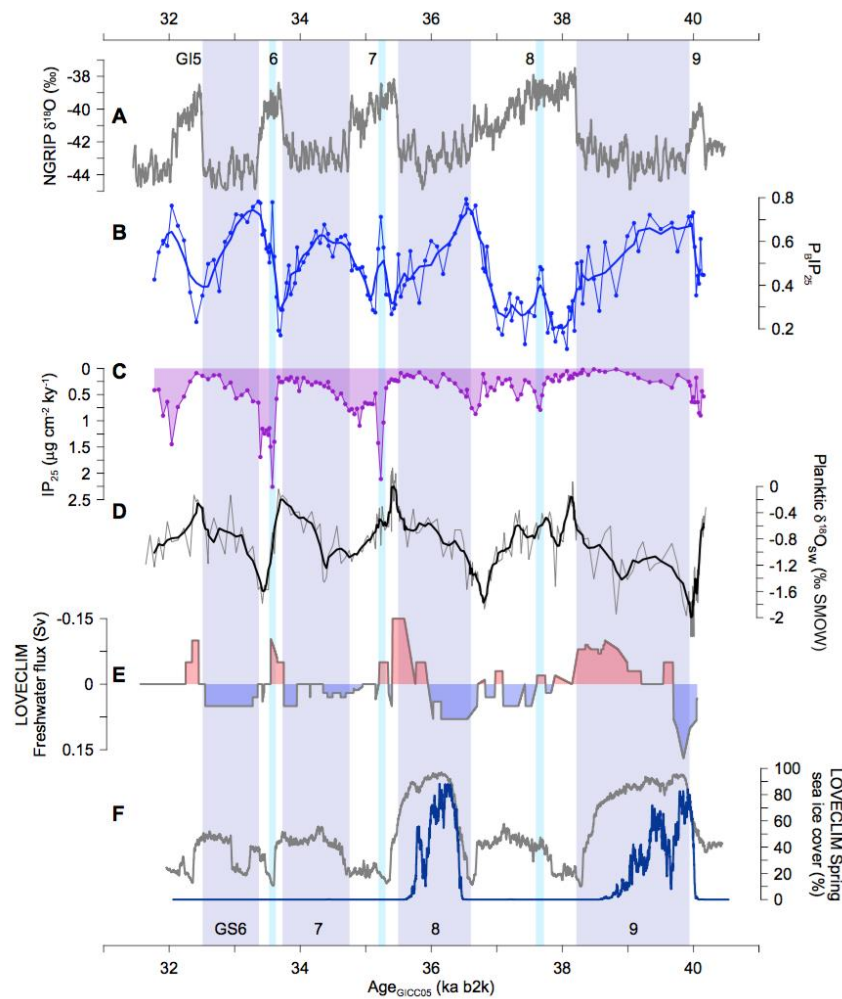


Fig. S4. Proxy-model data comparison. (A) NGRIP ice core $\delta^{18}\text{O}$ plotted as 11-point running average (2, 4). (B) $P_{\text{IP}_{25}}$. (C) IP_{25} flux. (D) Planktic $\delta^{18}\text{O}_{\text{SW}}$ based on planktic foraminiferal $\delta^{18}\text{O}$ corrected for changes in sea level/continental ice volume and near-surface temperature (14). (E) Freshwater flux applied as forcing in the transient D–O numerical experiment performed with the Earth system model LOVECLIM (9). (F) Simulated spring sea ice cover averaged over 60°N – 62.5°N , 1.25°W – 1.25°E (blue; core site) and 60°N – 80°N , 15°W – 20°E (gray; larger-scale Norwegian Sea) (9). All records are plotted on the GICC05 b2k timescale. Thick lines in (B) and (D), five-point running averages. GI, Greenland interstadials numbered at top. GS, Greenland stadials numbered at bottom (shaded bars). Light blue bars, intra-interstadial sea ice expansion events.